

Message passing method for social contagion in hypergraphs

Hui Leng(冷卉), Zhao-Yan Wu(吴召艳), and Rong Wang(王荣)

Citation: Chin. Phys. B, 2026, 35 (**5**): 056403. DOI: 10.1088/1674-1056/ae5c73
http://cpb.iphy.ac.cn; http://iopscience.iop.org/cpb

What follows is a list of articles you may be interested in

Interparticle-friction-induced anomalous colloid structure

Fuzhou Liu(刘福洲), Yu Ding(丁宇), Longfei Li(黎龙飞), Ke Cheng(程可), Fangfu Ye(叶方富), and Mingcheng Yang(杨明成)
Chin. Phys. B, 2025, 34 (**1**): 016401. DOI: 10.1088/1674-1056/ad9300

Unveiling the early stage evolution of local atomic structures in the crystallization process of a metallic glass

Lin Ma(马琳), Xiao-Dong Yang(杨晓东), Feng Yang(杨锋), Xin-Jia Zhou(周鑫嘉), and Zhen-Wei Wu(武振伟)
Chin. Phys. B, 2024, 33 (**3**): 036402. DOI: 10.1088/1674-1056/ad24d6

Nonvanishing optimal noise in cellular automaton model of self-propelled particles

Guang-Le Du(杜光乐) and Fang-Fu Ye(叶方富)
Chin. Phys. B, 2022, 31 (**8**): 086401. DOI: 10.1088/1674-1056/ac67c4

Improving robustness of complex networks by a new capacity allocation strategy

Jun Liu(刘军)
Chin. Phys. B, 2021, 30 (**1**): 016401. DOI: 10.1088/1674-1056/abb3f1

Analysis of overload-based cascading failure in multilayer spatial networks

Min Zhang(张敏), Xiao-Juan Wang(王小娟), Lei Jin(金磊), Mei Song(宋梅), Zhong-Hua Liao(廖中华)
Chin. Phys. B, 2020, 29 (**9**): 096401. DOI: 10.1088/1674-1056/aba275

Message passing method for social contagion in hypergraphs

Hui Leng(冷卉)[1,†], Zhao-Yan Wu(吴召艳)[2], and Rong Wang(王荣)[1]

[1] *School of Applied Mathematics, Shanxi University of Finance and Economics, Taiyuan* 030006, *China*
[2] *School of Mathematics and Statistics, Jiangxi Normal University, Nanchang* 330022, *China*

(Received 5 January 2026; revised manuscript received 23 March 2026; accepted manuscript online 8 April 2026)

The emergence of hypergraphs has solved the problem that the interactions between nodes are insufficient to describe the complex relationships among multiple individuals. In this paper, we model social contagion with the reinforcement effect on hypergraphs, where hyperedges disseminate information to nodes, and nodes upload information to hyperedges. In order to reduce the complexity of high-order interactions on the propagation, hypergraphs are mapped to factor graphs, where hyperedges are encoded to factor nodes, and the connection between a node and a factor node indicates that the node is located in the hyperedge. Taking into account the heterogeneity of nodes and hyperedges, we establish the message passing evolution equations about each node based on the factor graph. Finally, we carry out numerical simulations by iterating the message passing equations. We find that the probability of the adopted state decreases before the outbreak of social contagion, and the final adopting scale suddenly increases as the transmission rates increase, which are caused by the combined action of high-order interactions and the social reinforcement effect. Significantly, the final adopting scale presents a step-like variation when the adopting threshold of hyperedges changes.

Keywords: social contagion, hypergraph, message passing method

PACS: 64.60.aq, 87.23.Kg

DOI: 10.1088/1674-1056/ae5c73 **CSTR:** 32038.14.CPB.ae5c73

1. Introduction

Complex networks are excellent tools for depicting pairwise interactions, where nodes represent individuals and edges denote the interactions between two individuals. However, a large amount of evidence indicates that there are not only pairwise interactions, but high-order interactions.[1,2] Hypergraphs provide a framework for characterizing high-order interactions, overcoming the limitation of complex networks in capturing such interactions.[3] In hypergraphs, a hyperedge can include any number of nodes, thereby depicting high-order interactions of the contained nodes. For example, a discussion group consisting of multiple members can be denoted by a hyperedge. Members conduct discussions and exchange ideas within the group. After making decisions, the group representative communicates with other groups and learns about their decisions. And then, the group representative conveys the information from other groups to the members of their own group.

As the mathematical theory of hypergraphs gradually becomes complete, the transmissions based on hypergraphs have also attracted attention.[4,5] In Ref. [6], Higham *et al.* focus on the SIS propagation model in a hypergraph, and analyze local stability and global stability via mean-field method. Liang *et al.* utilize tensor algebra to explore discrete-time SIS social contagion processes on weighted and directed hypergraphs in Ref. [7]. The presence of the higher-order interaction leads to the bistability. In social contagion, due to differences in cognitive levels, environmental factors, and other influences, individuals repeatedly verify the reliability of the received information and only accept it after multiple confirmations. It indicates that social contagion has a key feature — social reinforcement effect, which distinguishes it from epidemic spreading. Generally, social contagion with reinforcing effects is characterized by the threshold model.[8,9] However, high-order interactions make social contagion more complicated, which leads to the network-based threshold model being unable to fully capture high-order effects. To reduce the complexity of high-order interactions, researchers transform a hypergraph into a factor graph and they confirm that it is feasible.[10,11] In particular, Peng *et al.* utilize the factor graph to solve higher-order percolation based on the message passing method.[11] Furthermore, the message passing method can generate state evolutions of each node based on network topology.[12–15] And the approach introduces a variable representing the probability that neighbors fail to transmit behavioral information to nodes, thereby giving the approach an advantage in studying social contagion with reinforcing effects. Therefore, among the numerous methods of propagation modeling, the message passing method is an effective way to formulate network-based social contagion.

Motivated by the above discussions, we focus on social contagion with the reinforcing effects on hypergraphs. Firstly, we transfer the propagation on the hypergraph to a factor graph, where hyperedges are mapped into factor nodes,

[†]Corresponding author. E-mail: huileng@sxufe.edu.cn

© 2026 Chinese Physical Society and IOP Publishing Ltd. All rights, including for text and data mining, AI training, and similar technologies, are reserved.

thereby facilitating the use of the message passing method to solve the propagation under high-order interactions. And then, a model is built to characterize the propagation. Further, after defining 'message' variables between nodes and factor nodes, we establish the message passing equations to derive state evolutions of each node by the message passing method. Finally, numerical simulations are carried out to observe the time evolution of social contagion and the changes of the final adopting scale under different transmission rates. And the relationships between the final adopting scale and adoption thresholds are also demonstrated.

On the whole, the contributions of this work are as follows. We construct a model on hypergraphs for social contagion dynamics with reinforcement effect, where the underlying propagation structures are expanded from pairwise interactions between two nodes to high-order interactions formed by multiple nodes. In the model, the occurrences of social contagion rely on propagation among nodes and hyperedges, and not only nodes but also hyperedges are in one of unadopted, adopted and recovery states at each time. When the amount of received information reaches their own adoption thresholds, the unadopted node and factor node become the adopted state, thereby reflecting the social reinforcement effect on nodes and hyperedges. The recovery state of a factor node is determined by whether the proportion of the number of recovery nodes contained in the hyperedge reaches the state threshold. Further, taking into account the heterogeneity of nodes and hyperedges, the node-based evolutions are formulated by the message passing evolution equations. It is confirmed that the message passing evolution equations are consistent with the Monte Carlo results, thereby providing an accurate model for characterizing social propagation in hypergraphs. And significantly, under the combined action of high-order interactions and social reinforcement effect, the probability of nodes in the adopted state decreases before the outbreak of social contagion, and the final adopting scale undergoes a first-order phase transition as the transmission rates increases. What's more, the final adopting scale presents a step-like variation when the adopting threshold of hyperedges changes.

2. Model

In this paper, the basic propagation structure of social contagion is a hypergraph $H=(V,E)$, which consists of the node set $V=\{v_1,v_2,\ldots,v_N\}$ and the hyperedge set $E=\{\boldsymbol{e}_1,\boldsymbol{e}_2,\ldots,\boldsymbol{e}_n\}$. The number of nodes is $|V|=N$ and the hyperdegree of node i is the number of hyperedges including node i. Hyperedge $\boldsymbol{e}_j=\{v_{i_1},v_{i_2},\ldots,v_{i_p}\}$ is composed of p nodes $v_{i_1},v_{i_2},\ldots,v_{i_p}$, where p is referred to as the cardinality of hyperedge $\boldsymbol{e}_j$ and denoted by $|\boldsymbol{e}_j|=p$. In particular, the hypergraph degenerates into an ordinary network when the cardinalities of all hyperedges are 2. For example, as shown in Fig. 1(a), the hypergraph $H=(V,E)$ is composed of a set of 9 nodes $V=\{v_1,v_2,\ldots,v_9\}$ and a set of 5 hyperedges $E=\{\boldsymbol{e}_1,\boldsymbol{e}_2,\ldots,\boldsymbol{e}_5\}$, where hyperedges are $\boldsymbol{e}_1=\{v_1,v_2\}$, $\boldsymbol{e}_2=\{v_2,v_3,v_4\}$, $\boldsymbol{e}_3=\{v_3,v_4,v_8\}$, $\boldsymbol{e}_4=\{v_1,v_4,v_5,v_6,v_7\}$ and $\boldsymbol{e}_5=\{v_8,v_9\}$.

In order to facilitate analysis of social contagion on a hypergraph by the message passing method, we convert the hypergraph $H=(V,E)$ into a factor graph $\mathcal{H}=(\mathcal{V},\mathcal{U},\mathcal{E})$. The set $\mathcal{V}$ denotes the set of nodes, consisting of all nodes in the hypergraph H. The set $\mathcal{U}$ denotes the set of factor nodes and each hyperedge in the hypergraph H represents a factor node. The set $\mathcal{E}$ represents all edges between nodes and factor nodes. If a hyperedge contains some nodes in the hypergraph, these nodes and the factor node will accordingly connect, thereby forming edges in the factor graph. As shown in Fig. 1(b), the hypergraph in Fig. 1(a) is transformed into a factor graph, where the sets of nodes and factor nodes are $\mathcal{V}=V$ and $\mathcal{U}=E$, respectively, and the set of edges $\mathcal{E}$ is composed of connecting lines between each hyperedge and contained nodes. For example, the hyperedge $\boldsymbol{e}_3$ in Fig. 1(a) contains nodes v_3, v_4 and v_8. According to the conversion rule, the lines connecting factor node $\boldsymbol{e}_3$ to nodes v_3, v_4 and v_8 are the edges in the factor graph in Fig. 1(b).

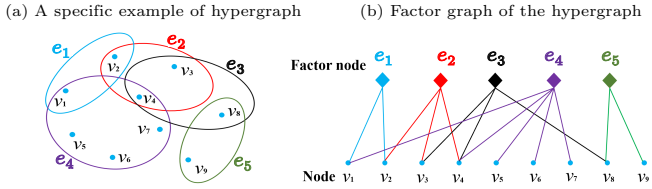


Fig. 1. (a) Hypergraph $H=(V,E)$ is composed of a set of 9 nodes $V=\{v_1,v_2,\ldots,v_9\}$ and a set of 5 hyperedges $E=\{\boldsymbol{e}_1,\boldsymbol{e}_2,\ldots,\boldsymbol{e}_5\}$, where 5 pieces of hyperedges are $\boldsymbol{e}_1=\{v_1,v_2\}$, $\boldsymbol{e}_2=\{v_2,v_3,v_4\}$, $\boldsymbol{e}_3=\{v_3,v_4,v_8\}$, $\boldsymbol{e}_4=\{v_1,v_4,v_5,v_6,v_7\}$ and $\boldsymbol{e}_5=\{v_8,v_9\}$. (b) Hypergraph $H=(V,E)$ is converted into a factor graph.

At each time, each node is in one of the unadopted, adopted and recovery states (U, A and R for short), and the same applies to each factor node. Node i being in the unadopted state implies that it has not adopted the behavior. Meanwhile, unadopted node i can receive the behavioral information from the adopted hyperedge $\boldsymbol{e}$ to which node i belongs, but it cannot transmit any information about the behavior. The nodes have memory for information and can remember the amount of received information. Node i adopts the behavior and simultaneously transforms from the unadopted state to the adopted state when the amount of information received from the adopted factor nodes connected to it is equal to or greater than the adoption threshold Y. And then, node i transmits behavioral information to the unadopted factor nodes connected with it at a certain rate β. After adopting the behavior, node i loses interest in the behavior at a rate γ and is unwilling to spread behavioral information anymore, thereby entering into the recovery state. If all nodes become the recovery state, the

propagation process will stop. Hyperedge e enters the adopted state from the unadopted state when the amount of information uploaded from nodes contained in hyperedge e is equal to or greater than adopting threshold of hyperedge e, and then it propagates information to unadopted nodes in hyperedge e at a rate β_e. In the model, the adopting thresholds for hyperedges with different numbers of nodes are diverse and are positively correlated with the number of containing nodes. We set hyperedge e's adopting threshold $Y_e^A = \lceil T_a|e| \rceil$ ($\lceil\cdot\rceil$ denotes round up to an integer), where T_a is the adopting threshold proportion of nodes in the hyperedge and its range of values is $[0,1]$. If the number of recovery nodes in hyperedge e is equal to or greater than $Y_e^R = \lceil T_r|e| \rceil$ (T_r is the proportion of recovery nodes in the hyperedge and its range of values is $[0,1]$), it will be in the recovery state.

For example, as shown in Fig. 2(a), nodes v_4, v_8 and v_9 are in the unadopted state, which are denoted by blue dots. Nodes v_1, v_2, v_3 are in the adopted state (red dots in Fig. 2(a)) and nodes v_5, v_6, v_7 are in the recovery state (black dots in Fig. 2(a)). In Fig. 2(b), the adopted node v_1 propagates the information to factor node e_1 (green line), but node v_2 does not pass the information to factor node e_1 (purple line). Then, let $T_a = T_r = 0.5$ and we calculate $Y_{e_1}^A = \lceil T_a|e_1| \rceil = 1$. For hyperedge e_1, the amount of received information is 1, which is equal to $Y_{e_1}^A = 1$, therefore, factor node e_1 is in the adopted state (red rhombus). Similarly, factor node e_2 is also in the adopted state, so factor node e_2 can pass information to the unadopted node v_4 with a certain probability along the yellow edge in factor graph. On the contrary, in Fig. 2(c), factor node e_5 is in the unadopted state (blue rhombus). The number of the recovery nodes in hyperedge e_4 is 3, which is equal to $Y_{e_4}^R = \lceil T_r|e_4| \rceil = 3$. Thus, factor node e_4 is in the recovery state (black rhombus).

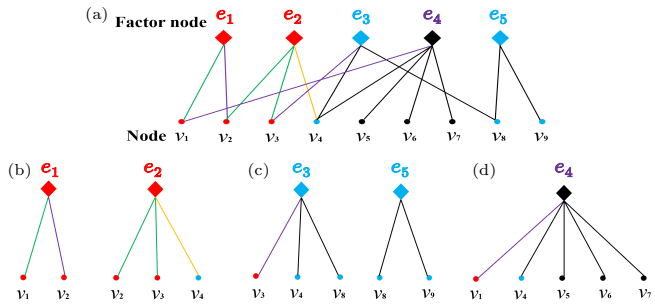


Fig. 2. A specific example of social contagion. The dots and rhombuses denote the nodes and factor nodes, respectively. The blue, red and black represent the unadopted, adopted and recovery states, respectively. The green lines indicate that the adopted nodes upload the information to the factor nodes. The purple lines indicate that the adopted nodes do not propagate the information to the factor nodes. And the yellow lines represent that the adopted factor nodes pass the information to the nodes with a certain probability.

3. Message passing equations

The state probability equations reflect the temporal evolution of each state under the transmission mechanism and serve as the basis for numerical simulations, implying that these equations play a key role in propagation studies. In this section, considering heterogeneities of nodes and hyperedges, we formulate node-based evolution equations through the message passing method. As an important quantity in the message passing method, 'message' is transmitted between the nodes and factor nodes. And to avoid repeating transmission of the information between node i and factor node e, we define 'message' $\tilde{\eta}_{e\to i}(t)$ as the probability that factor node e has not transmitted information to node i by time t and 'message' $\hat{\eta}_{k\to e}(t)$ as the probability that node k has not transmitted information to factor node e by time t. The initial values of $\tilde{\eta}_{e\to i}(0)$ and $\hat{\eta}_{k\to e}(0)$ are 1.

Let $\mathcal{T}_i(t)$ ($\mathcal{T} \in \{U,A,R\}$) be the probability of node i being in the $\mathcal{T}$ state at time t. If node i does not adopt the behavior at the initial time and the total number of information received from hyperedges to which node i belongs is less than the adoption threshold Y by time t, it will remain in the unadopted state. Based on the analysis, the dynamical equation of $U_i(t)$ is

$$U_i(t) = U_i(0) \sum_{\substack{S_e \subseteq E_i \\ |S_e|<Y}} \prod_{e\in S_e} (1-\tilde{\eta}_{e\to i}(t)) \prod_{d\in E_i\backslash S_e} \tilde{\eta}_{d\to i}(t), \quad (1)$$

where E_i is the set composed of the hyperedges to which node i belongs. S_e is the subset of E_i and $|\,S_e\,|$ denotes the size of S_e. $E_i\backslash S_e$ represents the complementary set of the subset S_e in E_i. The calculation of $U_i(t)$ is about probability, thus it is necessary to consider all possible combinations of subsets of E_i.

At time t, the hyperedge e is in any one of three states with a certain probability, and each state affects the information dissemination from hyperedge e to node i. Therefore, $\tilde{\eta}_{e\to i}(t)$ is determined by the state of hyperedge e, that is,

$$\tilde{\eta}_{e\to i}(t) = \tilde{\xi}^U_{e\to i}(t) + \tilde{\xi}^A_{e\to i}(t) + \tilde{\xi}^R_{e\to i}(t), \quad (2)$$

where $\tilde{\xi}^{\mathcal{T}}_{e\to i}(t)$ ($\mathcal{T} \in \{U,A,R\}$) denotes the probability that hyperedge e is in $\mathcal{T}$ state and has not transmitted the information to node i at time t.

When hyperedge e is in the unadopted state at time t, hyperedge e has not adopted the behavior, and thus cannot propagate the behavioral information to node i. Thus, $\tilde{\xi}^U_{e\to i}(t)$ is equal to the probability that hyperedge e is in the unadopted state at time t,

$$\tilde{\xi}^U_{e\to i}(t) = \sum_{\substack{S_k \subseteq N_e\backslash\{i\} \\ |S_k|<Y_e^A}} \prod_{k\in S_k} (1-\hat{\eta}_{k\to e}(t)) \prod_{j\in N_e\backslash(S_k\cup\{i\})} \hat{\eta}_{j\to e}(t), \quad (3)$$

where N_e is the set of all nodes contained in hyperedge e, and $N_e\backslash\{i\}$ is the set N_e excluding node i. S_k is the subset of $N_e\backslash\{i\}$, and $|\,S_k\,|$ represents the size of the set S_k. $N_e\backslash(S_k\cup\{i\})$ denotes the complementary set of the set $S_k\cup\{i\}$ in N_e, i.e., the set of the nodes contained in hyperedge e excepting for the nodes in the set S_k and node i. The purpose of

removing node i is to prevent repeated propagation between factor node $\boldsymbol{e}$ and node i, and consider the dynamical correlations between the states of the nodes and factor nodes. $\tilde{\xi}^{U}_{\boldsymbol{e}\to i}(t)$ is the cavity probability, thereby avoiding the echo chamber effect.

When factor node $\boldsymbol{e}$ is in the adopted state, the information transmission from factor node $\boldsymbol{e}$ to node i at time t causes the decrease of $\tilde{\eta}_{\boldsymbol{e}\to i}(t)$. Thus, the derivative of $\tilde{\eta}_{\boldsymbol{e}\to i}(t)$ is

$$\frac{\mathrm{d}\tilde{\eta}_{\boldsymbol{e}\to i}(t)}{\mathrm{d}t} = -\beta_{\boldsymbol{e}}\tilde{\xi}^{A}_{\boldsymbol{e}\to i}(t). \tag{4}$$

However, if factor node $\boldsymbol{e}$ in the adopted state has not transmitted information to node i and changes to the recovery state at time t, it will cause the increase of $\tilde{\xi}^{R}_{\boldsymbol{e}\to i}(t)$. The dynamical change of $\tilde{\xi}^{R}_{\boldsymbol{e}\to i}(t)$ is expressed as

$$\frac{\mathrm{d}\tilde{\xi}^{R}_{\boldsymbol{e}\to i}(t)}{\mathrm{d}t} = \gamma_{\boldsymbol{e}}(1-\beta_{\boldsymbol{e}})\tilde{\xi}^{A}_{\boldsymbol{e}\to i}(t), \tag{5}$$

where $\gamma_{\boldsymbol{e}} = \sum_{\substack{S_k\subseteq N_{\boldsymbol{e}}\\ |S_k|<Y^{R}_{\boldsymbol{e}}}} \prod_{k\in S_k} R_k(t)$ is the recovery rate of factor node $\boldsymbol{e}$.

Equation (4) is transformed into $\tilde{\xi}^{A}_{\boldsymbol{e}\to i}(t) = -\frac{\mathrm{d}\tilde{\eta}_{\boldsymbol{e}\to i}(t)}{\beta_{\boldsymbol{e}}\,\mathrm{d}t}$, and we substitute it into Eq. (5),

$$\frac{\mathrm{d}\tilde{\xi}^{R}_{\boldsymbol{e}\to i}(t)}{\mathrm{d}t} = -\frac{\gamma_{\boldsymbol{e}}(1-\beta_{\boldsymbol{e}})}{\beta_{\boldsymbol{e}}} \times \frac{\mathrm{d}\tilde{\eta}_{\boldsymbol{e}\to i}(t)}{\mathrm{d}t}. \tag{6}$$

Integrating both sides of Eq. (6) over the interval $[0,t]$, and using the initial conditions $\tilde{\xi}^{R}_{\boldsymbol{e}\to i}(0)=0$, $\tilde{\eta}_{\boldsymbol{e}\to i}(0)=1$, we obtain

$$\tilde{\xi}^{R}_{\boldsymbol{e}\to i}(t) = \gamma_{\boldsymbol{e}}(1-\frac{1}{\beta_{\boldsymbol{e}}})(\tilde{\eta}_{\boldsymbol{e}\to i}(t)-1). \tag{7}$$

Substituting Eqs. (2), (3) and (7) into Eq. (4), we get

$$\begin{aligned}\frac{\mathrm{d}\tilde{\eta}_{\boldsymbol{e}\to i}(t)}{\mathrm{d}t} &= \beta_{\boldsymbol{e}}\left[\tilde{\xi}^{U}_{\boldsymbol{e}\to i}(t) - \tilde{\eta}_{\boldsymbol{e}\to i}(t)\right]\\ &\quad +\gamma_{\boldsymbol{e}}(1-\beta_{\boldsymbol{e}})(1-\tilde{\eta}_{\boldsymbol{e}\to i}(t)).\end{aligned} \tag{8}$$

Similar to the calculation of $\tilde{\eta}_{\boldsymbol{e}\to i}(t)$, $\hat{\eta}_{k\to\boldsymbol{e}}(t)$ is determined by the state of node k at time t, and thus it is calculated in three parts. That is, $\hat{\eta}_{k\to\boldsymbol{e}}(t) = \hat{\xi}^{U}_{k\to\boldsymbol{e}}(t) + \hat{\xi}^{A}_{k\to\boldsymbol{e}}(t) + \hat{\xi}^{R}_{k\to\boldsymbol{e}}(t)$. The probabilities that node k is in U, A, R states and has not transmitted information to the associated hyperedge $\boldsymbol{e}$ by time t are represented by $\hat{\xi}^{U}_{k\to\boldsymbol{e}}(t)$, $\hat{\xi}^{A}_{k\to\boldsymbol{e}}(t)$, and $\hat{\xi}^{R}_{k\to\boldsymbol{e}}(t)$, respectively.

The probability $\hat{\xi}^{U}_{k\to\boldsymbol{e}}(t)$ is equal to the probability that node k is in the unadopted state at time t. The information transmission is nonredundant in the message passing method. Therefore, when we traverse the hyperedges to which node k belongs, the hyperedge $\boldsymbol{e}$ should be excluded.

$$\begin{aligned}\hat{\xi}^{U}_{k\to\boldsymbol{e}}(t) &= U_k(0) \sum_{\substack{S_{\boldsymbol{m}}\subseteq E_k\setminus\{\boldsymbol{e}\}\\ |S_{\boldsymbol{m}}|<Y}} \prod_{\boldsymbol{m}\in S_{\boldsymbol{m}}} (1-\tilde{\eta}_{\boldsymbol{m}\to k}(t))\\ &\quad \times \prod_{\boldsymbol{h}\in E_k\setminus(S_{\boldsymbol{m}}\cup\{\boldsymbol{e}\})} \tilde{\eta}_{\boldsymbol{h}\to k}(t),\end{aligned} \tag{9}$$

where E_k is the hyperedge set to which node k belongs, $S_{\boldsymbol{m}}$ is the subset of E_k and its size is $|\,S_{\boldsymbol{m}}\,|$. Similar to the analysis of Eqs. (4), (5) and (8), we obtain

$$\begin{aligned}\frac{\mathrm{d}\hat{\eta}_{k\to\boldsymbol{e}}(t)}{\mathrm{d}t} &= \beta\left[\hat{\xi}^{U}_{k\to\boldsymbol{e}}(t) - \hat{\eta}_{k\to\boldsymbol{e}}(t)\right]\\ &\quad +\gamma(1-\beta)(1-\hat{\eta}_{k\to\boldsymbol{e}}(t)).\end{aligned} \tag{10}$$

At time t, if the unadopted node i enters the adopted state, it will lead to an increase of $A_i(t)$. On the contrary, if the adopted node i recovers, it will reduce $A_i(t)$ and increase $R_i(t)$. The derivatives of $A_i(t)$ and $R_i(t)$ are expressed as

$$\frac{\mathrm{d}A_i(t)}{\mathrm{d}t} = -\frac{\mathrm{d}U_i(t)}{\mathrm{d}t} - \gamma A_i(t), \quad \frac{\mathrm{d}R_i(t)}{\mathrm{d}t} = \gamma A_i(t). \tag{11}$$

Equations (1), (3) and (8)–(10) provide the complete dynamical evolution equations of social contagion on hypergraphs, thereby calculating the state probabilities of the nodes at any time.

In addition, we also concern the condition under which the outbreak of social contagion occurs. As adopted nodes and factor nodes continuously transmit information, the 'messages' $\tilde{\eta}_{\boldsymbol{e}\to i}(t)$ and $\hat{\eta}_{k\to\boldsymbol{e}}(t)$ gradually decrease over time. By setting the right side of Eqs. (8) and (10) to be 0, the 'messages' $\tilde{\eta}_{\boldsymbol{e}\to i}(t)$ and $\hat{\eta}_{k\to\boldsymbol{e}}(t)$ cease to change, and the state variables $U_i(t)$, $A_i(t)$ and $R_i(t)$ reach their steady states. Accordingly, we obtain

$$\begin{aligned}\tilde{\eta}_{\boldsymbol{e}\to i}(\infty) &= \frac{\gamma_{\boldsymbol{e}}(1-\beta_{\boldsymbol{e}})(1-\tilde{\eta}_{\boldsymbol{e}\to i}(\infty))}{\beta_{\boldsymbol{e}}} + \tilde{\xi}^{U}_{\boldsymbol{e}\to i}(\infty),\\ \hat{\eta}_{k\to\boldsymbol{e}}(\infty) &= \frac{\gamma(1-\beta)(1-\hat{\eta}_{k\to\boldsymbol{e}}(\infty))}{\beta} + \hat{\xi}^{U}_{k\to\boldsymbol{e}}(\infty).\end{aligned} \tag{12}$$

The outbreak threshold corresponds to the conditions under which the trivial solution emerges in Eq. (12), that is, the point at which functions

$$\begin{aligned}g &= -\tilde{\eta}_{\boldsymbol{e}\to i}(\infty) + \frac{\gamma_{\boldsymbol{e}}(1-\beta_{\boldsymbol{e}})(1-\tilde{\eta}_{\boldsymbol{e}\to i}(\infty))}{\beta_{\boldsymbol{e}}} + \tilde{\xi}^{U}_{\boldsymbol{e}\to i}(\infty),\\ f &= -\hat{\eta}_{k\to\boldsymbol{e}}(\infty) + \frac{\gamma(1-\beta)(1-\hat{\eta}_{k\to\boldsymbol{e}}(\infty))}{\beta} + \hat{\xi}^{U}_{k\to\boldsymbol{e}}(\infty)\end{aligned}$$

are tangent to horizontal axis at the critical values of $\tilde{\eta}^{\mathrm{c}}_{\boldsymbol{e}\to i}(\infty)$, $\hat{\eta}^{\mathrm{c}}_{k\to\boldsymbol{e}}(\infty)$, and

$$\begin{aligned}\frac{\mathrm{d}g(\tilde{\eta}_{\boldsymbol{e}\to i}(\infty),\hat{\eta}_{k\to\boldsymbol{e}}(\infty))}{\mathrm{d}\tilde{\eta}_{\boldsymbol{e}\to i}(\infty)}\Big|_{\tilde{\eta}^{\mathrm{c}}_{\boldsymbol{e}\to i}(\infty)} &= 0,\\ \frac{\mathrm{d}f(\tilde{\eta}_{\boldsymbol{e}\to i}(\infty),\hat{\eta}_{k\to\boldsymbol{e}}(\infty))}{\mathrm{d}\hat{\eta}_{k\to\boldsymbol{e}}(\infty)}\Big|_{\hat{\eta}^{\mathrm{c}}_{k\to\boldsymbol{e}}(\infty)} &= 0.\end{aligned}$$

Through further calculations, the outbreak thresholds are

$$\begin{aligned}\beta^{\mathrm{c}}_{\boldsymbol{e}} &= \frac{\gamma_{\boldsymbol{e}}}{\frac{\mathrm{d}\tilde{\xi}^{U}_{\boldsymbol{e}\to i}(\infty)}{\mathrm{d}\tilde{\eta}_{\boldsymbol{e}\to i}(\infty)}\big|_{\tilde{\eta}^{\mathrm{c}}_{\boldsymbol{e}\to i}(\infty)} + \gamma_{\boldsymbol{e}} - 1},\\ \beta^{\mathrm{c}} &= \frac{\gamma}{\frac{\mathrm{d}\hat{\xi}^{U}_{k\to\boldsymbol{e}}(\infty)}{\mathrm{d}\hat{\eta}_{k\to\boldsymbol{e}}(\infty)}\big|_{\hat{\eta}^{\mathrm{c}}_{k\to\boldsymbol{e}}(\infty)} + \gamma - 1}.\end{aligned} \tag{13}$$

At first glance, the transmission rate β appears to be unrelated to the outbreak threshold β_e^c. However, $\tilde{\xi}^U_{e\to i}(\infty)$ is computed based on $\hat{\eta}_{k\to e}(\infty)$ and β from Eqs. (3) and (10), indicating that β_e^c is related to β. Similarly, β^c is associated with β_e. Therefore, in essence, the values of the transmission rates β_e and β have substantial impacts on the outbreak thresholds. The outbreak threshold represents the critical point at which a phase transition occurs in social contagion dynamics. When both transmission rates β and β_e exceed their respective outbreak thresholds, social contagion widely spreads and the final adoption scale $R(\infty)$ gradually increases.

4. Numerical illustrations

Based on the above message passing evolutions of each node in Section 3, we conduct numerical simulations on an artificial hypergraph, Karate hypergraph and scale-free hypergraph. The artificial hypergraph and the Karate hypergraph are shown in Figs. 3(a) and 3(b), respectively. The Karate hypergraph is constructed based on the training schedules of the members in the Karate club, where members who are trained at the same time form a hyperedge.[16] There are 14 hyperedges, which are shown in Table 1. The scale-free hypergraph consists of 1000 nodes and is characterized by a power-law exponent of 2.2, an average node hyperdegree of 4.5, and an average hyperedge size of 9. The topology of the artificial hypergraph is presented in the matrix $\mathcal{A}$, where the row and column denote the nodes and hyperedges, respectively. If node i is in hyperedge e, then $\mathcal{A}(i,e)$ is equal to 1, otherwise, $\mathcal{A}(i,e)=0$. Matrix $\mathcal{A}$ is also the topology of the factor graph corresponding to the hypergraph, where the row and column denote the nodes and factor nodes, respectively. The Karate hypergraph and scale-free hypergraph are similarly transformed, thereby yielding their factor graph.

$$\mathcal{A}=\begin{bmatrix}
0&0&0&0&0&0&1&0&1&1&1&0&0&0&1&0&0&0&1&0\\
0&1&1&0&0&0&0&1&0&0&0&1&1&0&1&1&1&0&0&0\\
1&0&1&1&1&0&0&0&0&0&1&0&0&1&0&0&0&0&1&0\\
0&1&0&0&1&1&0&1&0&0&0&0&1&1&1&0&0&0&1&0\\
0&1&0&1&1&0&0&0&0&1&0&1&0&1&0&0&1&0&0&1\\
0&0&0&0&1&0&0&0&0&0&0&0&0&0&0&0&1&1&0&0\\
0&0&0&0&1&0&1&0&0&0&1&1&0&1&0&0&0&0&0&0\\
0&0&0&0&0&1&0&1&0&1&0&0&0&0&0&1&0&1&1&0\\
0&0&1&0&0&1&0&0&1&0&0&0&0&1&1&0&0&0&0&0\\
1&0&1&1&0&0&0&1&0&0&1&1&0&0&1&1&1&0&0&1
\end{bmatrix}.$$

The message passing evolutions in Section 3 indicate that its numerical calculation is an iterative solution process. The specific steps are as follows: (i) solving the differential Eqs. (8) and (10) according to ode45 algorithm, (ii) calculating the probabilities $\tilde{\xi}^U_{e\to i}(t)$ and $\hat{\xi}^U_{k\to e}(t)$, (iii) repeating steps (i) and (ii), and updating messages $\tilde{\eta}_{e\to i}$ and $\hat{\eta}_{k\to e}$ until convergence, (iv) calculating the state probability $U_i(t)$, $A_i(t)$ and $R_i(t)$. Consequently, the state evolutions of the nodes are obtained according to the above numerical calculations. In order to observe the overall effect, we take the average value of the state probability about all nodes as the observation target, i.e., $\mathcal{T}(t)=\frac{1}{N}\sum_{i=1}^{N}\mathcal{T}_i(t)$ $(\mathcal{T}\in\{U,A,R\})$. We set the initial values $U(0)=0.8$ and $I(0)=0.2$. In the simulations, we choose the recovery rate $\gamma=0.2$ and the adopting threshold of the node $Y=2$ in three hypergraphs, the adopting threshold proportions of nodes in the hyperedge $T_a=0.5$ in artificial hypergraph, $T_a=0.2$ in Karate hypergraph and scale-free hypergraph. And the proportions of recovery nodes are $T_r=0.5$ in artificial hypergraph and Karate hypergraph, $T_r=0.2$ in scale-free hypergraph.

Table 1. Hyperedges in Karate hypergraph.

Hyperedge	Nodes in hyperedge
e_1	15,16,17,18,19,20,21,22,23,24
e_2	9,10,25,26,27,28,29,30,31,32,33,34
e_3	1,2,3,4,5,6,7,8,11,12,13,14,15,16
e_4	1,3,5,7,9,11,13,25,27,29,31,33
e_5	1,2,3,4,9,10,13,14,25,26,31,32,33,34
e_6	1,2,3,4,5,6
e_7	34,9,10,29,30,31
e_8	20,21,22,23,24,25,26,27,28,29,30,31,32,33
e_9	1,2,3,4
e_{10}	34,9,10,31,32,33
e_{11}	5,6,7,8,11,12,13,14
e_{12}	15,16,14,18,19,20
e_{13}	21,22,23,24,25,26
e_{14}	27,28,29,30,31,32,33,34

(a) Artificial hypergraph (b) Karate hypergraph

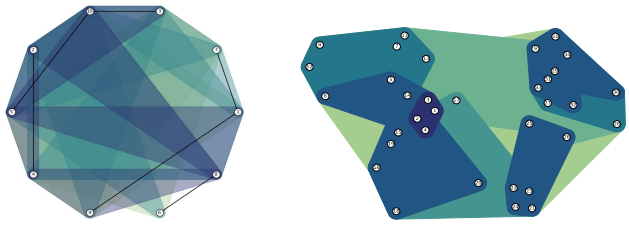


Fig. 3. Topologies of (a) artificial hypergraph and (b) Karate hypergraph.

Firstly, we illustrate the time evolutions of unadopted, adopted and recovery states under different transmission rates β, which are obtained under transmission rates $\beta_e=0.5$ in artificial hypergraph and Karate hypergraph, and $\beta_e=0.6$ in scale-free hypergraph. Figures 4(a) and 4(d) show the results in the artificial hypergraph under $\beta=0.2$ and 0.7, respectively. Figures 4(b) and 4(e) are about Karate hypergraph under $\beta=0.2$ and 0.8, respectively. Figures 4(c) and 4(f) are about scale-free hypergraph under $\beta=0.05$ and 0.4, respectively. Further, we verify the change rates of the unadopted and adopted states, as shown in the upper right corner of each subgraph in Fig. 4. It is obvious that $\mathrm{d}A(t)/\mathrm{d}t$ is initially negative and eventually equals 0 in Fig. 4(a), with the result that the curve of $A(t)$ keeps decreasing until it reaches 0 at $t=40$.

A similar trend is also observed in Figs. 4(b) and 4(c). The time evolutions of the adopted state in Figs. 4(a)–4(c) imply that social contagion does not break out and eventually comes to a halt. However, when $\beta = 0.7$, the value of $A(t)$ exceeds the initial value 0.2 for $t \in [4.5, 15]$ in Fig. 4(c) and reaches the peak values 0.35 at $t = 10$, which indicates that social contagion outbreaks. A similar phenomenon is also observed in Figs. 4(d) and 4(e). In Figs. 4(d)–4(f), a different pattern emerges: $\mathrm{d}A(t)/\mathrm{d}t$ becomes positive during a certain period of time. Specifically, it starts negative, then becomes positive. It later turns negative again, and finally reaches zero. Consequently, $A(t)$ exhibits a trajectory of decline, followed by rise, and then another decline, eventual stabilization. The fundamental reason is that during the initial stage of social contagion, the amount of received information for node and factor nodes does not reach the adoption thresholds, thereby most of nodes and factor nodes being in the unadopted state. Meanwhile, some nodes and factor nodes that are initially in the adopted state recover. That is, the rate at which $U(t)$ decreases is less than the rate at which adopted nodes become recovered (i.e., $-\mathrm{d}U(t)/\mathrm{d}t < \gamma A(t)$), and the change rate of the adopted state $\mathrm{d}A(t)/\mathrm{d}t = -\mathrm{d}U(t)/\mathrm{d}t - \gamma A(t) < 0$, thereby leading to decrease of $A(t)$. As the dissemination continues, the nodes and factor nodes gradually adopt the behavior, which causes $A(t)$ to gradually increase. Then the adopted nodes and factor nodes lose interest in the behavior and stop transmitting relevant information, thereby causing $A(t)$ to fall. Finally, all adopted nodes and factor nodes enter the recovery state, and the value of $A(t)$ remains 0, which implies the propagation stops. It is shown that, in all cases, the change rate of the unadopted state $\mathrm{d}U(t)/\mathrm{d}t \leq 0$, implying that $U(t)$ either decreases or remains unchanged. As is well known, based on the transmission mechanism and the expression of $R(t)$, the change rate of the recovery state throughout the entire transmission process is always greater than or equal to 0. Therefore, the probability of being in the recovery state either increases or remains unchanged.

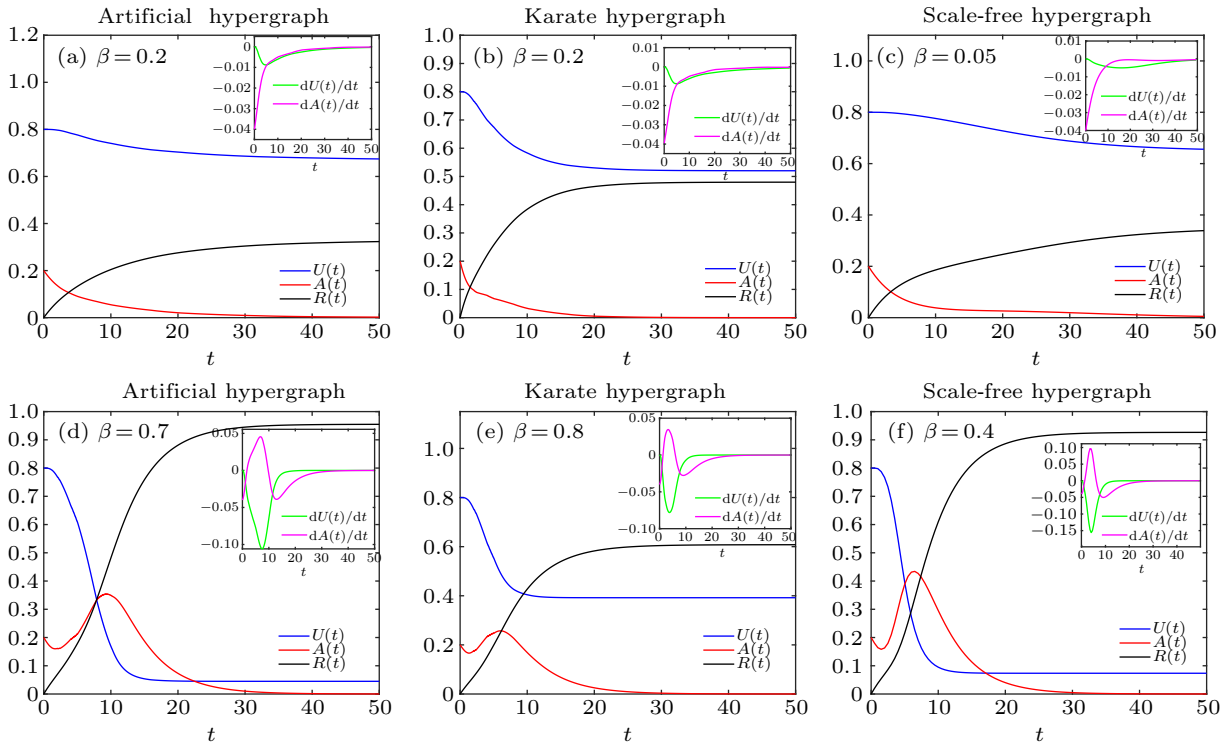


Fig. 4. The time evolutions of U, A and R states under different transmission rates β.

It is observed that the transmission rate influences the trend of state evolutions in Fig. 4. Then, we attempt to investigate the changes in the final adopting scale (i.e., stable state of R) with variations of transmission rates β and β_e, as shown in Figs. 5(a) and 5(b), respectively. In Fig. 5(a), we set $\beta_e = 0.5$ in artificial hypergraph, $\beta_e = 0.7$ in Karate hypergraph and $\beta_e = 0.1$ in scale-free hypergraph. In Fig. 5(b), we set $\beta = 0.2$ in artificial hypergraph, $\beta = 0.4$ in Karate hypergraph and $\beta = 0.1$ in scale-free hypergraph. On the whole, the final adopting scale $R(\infty)$ rises as β aggrandizes in Fig. 5(a). Tellingly, there is a sudden and saltatory increase in $R(\infty)$ at $\beta = 0.25$ in artificial hypergraph, $\beta = 0.15$ in Karate hypergraph and $\beta = 0.1$ in scale-free hypergraph, implying the occurrence of a first order transition. When the speed of information dissemination from nodes to factor nodes β is very small, both nodes and factor nodes are in the stage of accumulating information. As β increases, under the combined action of high-order interactions and social reinforcement ef-

fect, the amount of received information for nodes and factor nodes increases rapidly, thereby causing the adoption threshold to be reached quickly. As a consequence, a large number of nodes and factor nodes change from the unadopted state to the adopted state. Thus, the phenomenon is reflected in physics aspect as a sudden increase of the final adopting scale $R(\infty)$, indicating the occurrence of a first-order phase transition. Similarly, the final adopting scale $R(\infty)$ increases with β_e rising in Figs. 5(b) and the growth rate of $R(\infty)$ is relatively higher for $\beta_e \in [0.6, 0.8]$ in artificial hypergraph, $\beta_e \in [0.35, 0.6]$ in Karate hypergraph and $\beta_e \in [0.05, 0.3]$ in scale-free hypergraph. Further, when β and β_e change simultaneously, the final adopting scale $R(\infty)$ also shows a sudden increase in Figs. 5(c)–5(e).

Since the adopting thresholds determine the amount of received information when the nodes and factor nodes enter the adopted state, they play a crucial role in social contagion. Thus, we explore the effects of Y and T_a on the social contagion. We set $\beta = 0.2$, $\beta_e = 0.5$ in artificial hypergraph, $\beta = 0.5$, $\beta_e = 0.5$ in Karate hypergraph, and $\beta = 0.1$, $\beta_e = 0.4$ in scale-free hypergraph. In Fig. 6(a), when the adoption threshold of node Y changes from 1 to 3 in three hypergraphs, $R(\infty)$ has the sharp reduction. However, $R(\infty)$ remains unchanged when $Y \geq 4$. In the three hypergraphs, the hyperdegree of the majority of nodes is less than or equal to 3. When the adopting threshold Y exceeds 3, the amount of received information for the majority of nodes is unable to reach the adopting threshold Y and thus social contagion cannot propagate. In Fig. 6(b), as T_a increases, $R(\infty)$ stepwise declines and the sudden decline occurs at $T_a \in [0.3, 0.4]$ and [0.5,0.6] in the artificial hypergraph, $T_a \in [0.2, 0.3]$ in Karate hypergraph and $T_a \in [0.5, 0.6]$ in scale-free hypergraph. When $T_a \geq 0.6$, the value of $R(\infty)$ remains at 0.2.

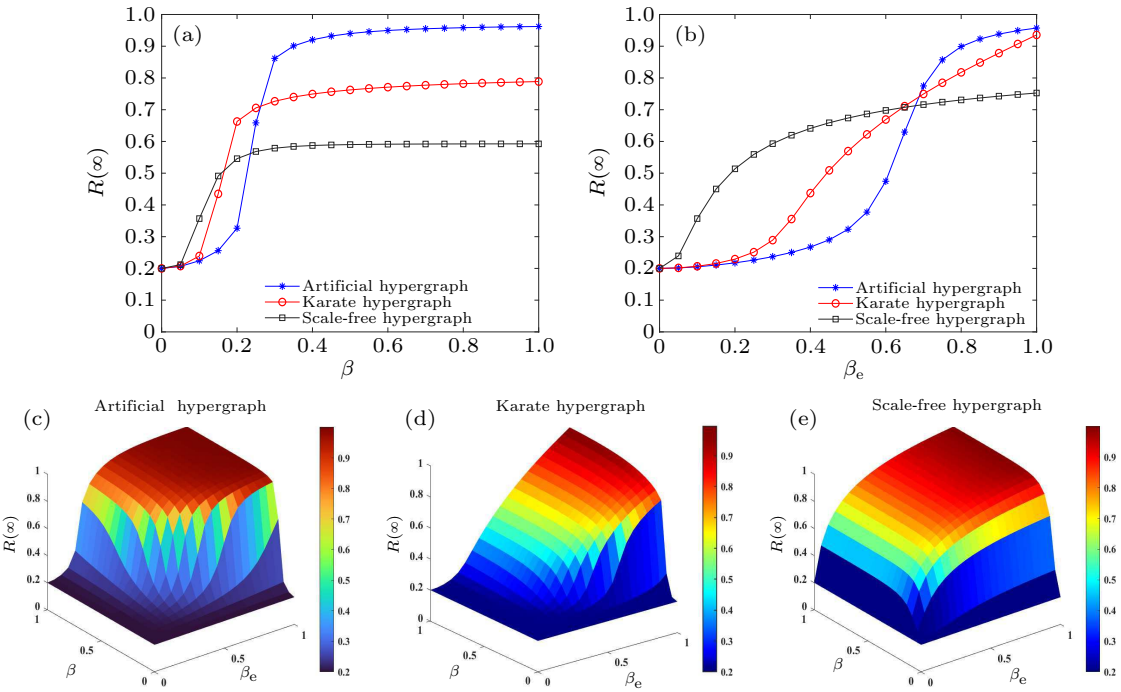


Fig. 5. The changes of the final adopting scale $R(\infty)$ with transmission rates β and β_e are shown in panels (a) and (b), respectively. The cases of β and β_e simultaneously changing in three hypergraphs are shown in panels (c)–(e), respectively.

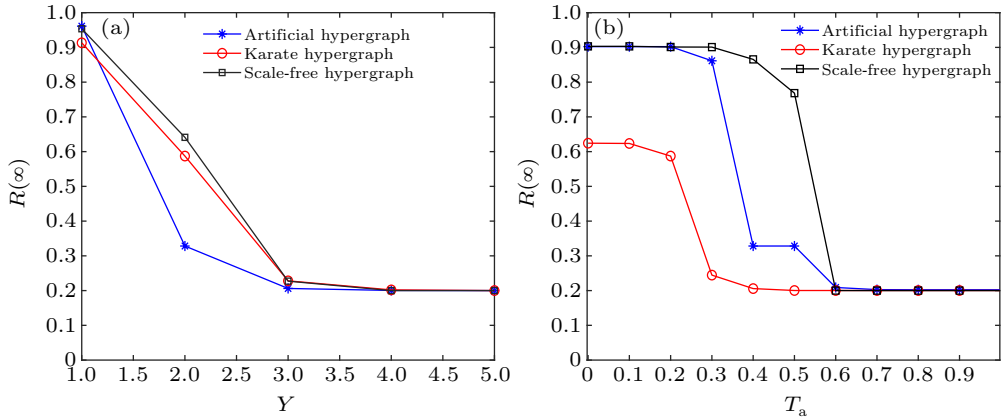


Fig. 6. The changes of the final adopting scale $R(\infty)$ with adoption thresholds Y and T_a are shown in panels (a) and (b), respectively.

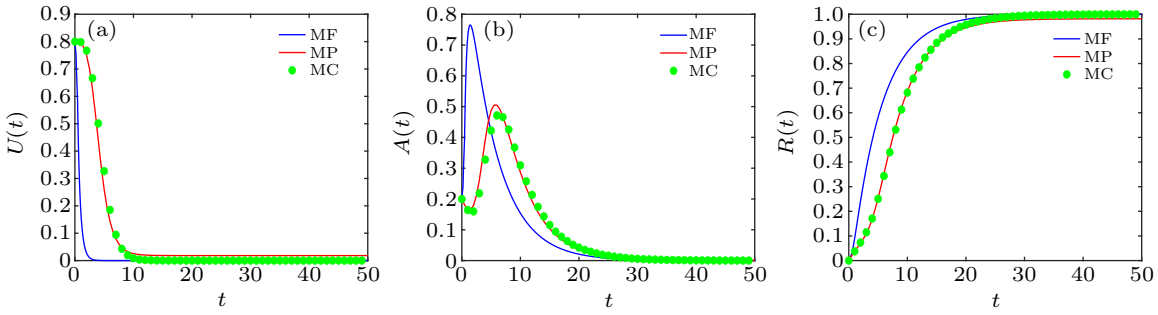


Fig. 7. The time evolutions of (a) U, (b) A and (c) R states under the mean-field approach (MF), Monte Carlo method (MC), and message passing method (MP).

Finally, we compare the temporal evolutions of social contagion in scale-free hypergraph predicted by the mean-field approach (MF), Monte Carlo method (MC), and message passing method (MP), as shown in Fig. 7. Here, we set $\beta = 0.4$, $\beta_{\boldsymbol{e}} = 0.9$. It is evident that the curves generated by MP align more closely with MC than MF. In particular, the trend of $A(t)$ under MF fails to capture the trend of initial decline, followed by a rise, another decline, and eventual stabilization, whereas both MP and MC successfully reproduce the tendency. It indicates that the message passing evolution equations developed in Section 3 more accurately characterize the social contagion on hypergraphs, thereby providing a precise mathematical model. The message passing evolution equations are constructed based on specific topological structure of hypergraphs and account for the heterogeneity of nodes and hyperedges, resulting in node-based evolution equations. In contrast, the mean-field evolution equations do not consider the detailed topology but instead rely on statistical hypergraph information, such as the hyperdegree distribution. On the other hand, MP avoids the echo chamber effect through introducing the cavity probability $\tilde{\xi}^{U}_{\boldsymbol{e}\to i}(t)$. That is, if a susceptible node i is infected by a hyperedge $\boldsymbol{e}$, the possibility of node i infecting hyperedge $\boldsymbol{e}$ is excluded. Even if the infection probability of node i is overestimated, it cannot affect hyperedge $\boldsymbol{e}$. And, in a sense, MP takes into account the dynamical correlations between the node and hyperedge states, and also avoids the redundant transmission of information between the nodes and hyperedges. Therefore, the message passing evolution equations in Section 3 offer a comprehensive description of social contagion in hypergraphs and achieve high accuracy, granting them a distinct advantage in predictive performance.

5. Conclusion

In this paper, social contagion based on hypergraphs is investigated, which aims at modeling complex social dissemination with the reinforcing effects under high-order interactions. The high-order interactions cause the formation of hyperedges consisting of multiple nodes, resulting in significant effects on transmission. Based on the hypergraphs, the information propagates between the nodes and hyperedges. The nodes and hyperedges have their own adopting thresholds. Each hyperedge is in one of the unadopted, adopted and recovery states at each time, and each node is as well. An unadopted hyperedge receives information from its containing nodes. If the accumulated quantity reaches the adopting threshold, the hyperedge will enter the adopted state. The hyperedge's recovery state is determined by the number of recovery nodes it contains. Each unadopted node receives information from its affiliated hyperedges, and enters the adopted state when the amount of information reaches the adopting threshold. The adopted nodes report the information to their affiliated hyperedges. When the adopted nodes lose interest about the information, they enter the recovery state. Further, we resort to the factor graph for reducing the complexity of high-order interactions in social contagion. Taking into account the heterogeneity of nodes and hyperedges, we define 'message' among different factor nodes and nodes, thereby deriving node-based state evolution equations based on the message passing method. And the evolution equations coincide with Monte Carlo method. Finally, we perform numerical solutions through iterating the message passing equations, thereby carrying out numerical simulations. The time evolution curves of three states under different transmission rates are obtained, including the outbreak and non-outbreak scenarios. Before the outbreak of social contagion, the probability of the adopted state decreases, caused by the combined action of high-order interactions and social reinforcement effects. It also leads to the situation that the final adopting scale suddenly increases when the transmission rates change. More significantly, as the adopting threshold of the hyperedges increases, the final adopting scale exhibits a step-like variation.

Acknowledgments

Project supported by the National Natural Science Foundation of China (Grant No. 61963019), Fundamental Research Program of Shanxi Province (Grant No. 202403021212007), Project of Shanxi Provincial Department of Education (Grant No. J20250117), and research funds of Shanxi University of Finance and Economics (Grant No. Z18428).

References

[1] Iacopini I, Petri G, Barrat A and Latora V 2019 *Nat. Commun.* **10** 2485
[2] Lu J T, Zhang J L, Xue Q, Zhao S Q, Liu Y N, Cui L Q and Meng F Y 2025 *Physica A* **678** 130947
[3] Ghoshal G, Zlatic V, Caldarelli G and Newman M E J 2009 *Phys. Rev. E* **79** 066118
[4] Ma Y, Xue X, Cai M and Wang W 2020 *Chin. Phys. B* **29** 128902
[5] Nian F and Zhang X 2023 *Chin. Phys. B* **32** 038901
[6] Higham D J and Kergorlay H L D 2022 *SIAM J. Appl. Math.* **82** 1987
[7] Liang L D, Cui S X and Liu F Z 2025 *IEEE T. Automat. Contr.* **71** 1114
[8] Granovetter M S 1978 *Am. J. Sociol.* **83** 1420
[9] Granovetter M S and Soong R 1983 *J. Math. Sociol.* **9** 165
[10] Sun H and Bianconi G 2021 *Phys. Rev. E* **104** 034306
[11] Peng H, Qian C, Zhao D D, Zhong M, Han J M, Zhou T and Wang W 2024 *Physica A* **634** 129446
[12] Karrer B and Newman M 2010 *Phys. Rev. E* **82** 016101
[13] Shrestha M and Moore C 2014 *Phys. Rev. E* **89** 022805
[14] Newman M E J 2023 *P. Roy. Soc. A-Math. Phy.* **479** 20220774
[15] Leng H, Zhao Y and Wang D 2022 *Physica A* **587** 126510
[16] Zachary W W 1977 *J. Anthropol. Res.* **33** 452